

Accuracy Considerations of Time-Splitting Methods for Models Using Two-Time-Level Schemes

R. JAMES PURSER

*Science Applications International Corporation, Beltsville, and NOAA/NCEP/Environmental Modeling Center,
Camp Springs, Maryland*

(Manuscript received 13 December 2005, in final form 3 July 2006)

1. Introduction

In their recent paper, Wicker and Skamarock (2002, hereafter WS) describe a novel adaptation of a time-splitting method (Klemp and Wilhelmson 1978) for integrating the elastic equations but applied to a basic explicit time integration scheme of Runge–Kutta type. The basis for their time integration method is an explicit three-stage, one-step (two time level) scheme that they refer to as a “third-order Runge–Kutta” scheme. The conventional second-order Runge–Kutta and Adams–Bashforth schemes are both formally unstable when applied to pure oscillatory linear modes without artificial damping (Gear 1971). The explicit but economical “leapfrog” or “midpoint” method is unstable for damped modes and, in practice, requires the intervention of a time filter (Asselin 1972) to control the otherwise undamped computational “parasitic” mode in wave simulations. The method of WS, in contrast, has excellent properties of stability for both oscillatory and damped modes and, with the splitting method they propose, permits the efficient integration of a fully elastic and nonhydrostatic atmospheric model. However, as we show below, a careful analysis of the basic method they propose upon which they build their splitting scheme reveals that it is not strictly accurate to third order (except for the very special case of purely linear dynamics, where its response *does* exactly match that of any true three-stage third-order Runge–Kutta method) but is better thought of as a three-stage second-order method with superior characteristics of stability and accuracy. While alternative fully third-order schemes of

Runge–Kutta type are discussed, the difficulties of combining these with robust splitting methods may preclude their practical implementation in numerical weather prediction models.

2. Accuracy of multistage one-step schemes

For simple dynamics,

$$\frac{d\boldsymbol{\psi}}{dt} = \mathbf{f}(\boldsymbol{\psi}, t), \quad (2.1)$$

in which a vector $\boldsymbol{\psi}$ of state variables evolves in response to a corresponding forcing \mathbf{f} , which is some function of both $\boldsymbol{\psi}$ and the time t , a three-stage, one-step integration scheme will update the state $\boldsymbol{\psi}$ over a complete time step Δt , from time t_0 to time $t_0 + \Delta t$, by the following stages, which we can express in notation similar to that of Butcher (1987):

$$\mathbf{Y}_i = \boldsymbol{\psi}(t_0) + \Delta t \sum_{j=1}^3 a_{ij} \mathbf{f}(\mathbf{Y}_j, t_0 + c_j \Delta t),$$

$$i = 1, 2, 3, \quad (2.2a)$$

$$\boldsymbol{\psi}(t_0 + \Delta t) \approx \mathbf{Y} = \boldsymbol{\psi}(t_0) + \Delta t \sum_{j=1}^3 b_j \mathbf{f}(\mathbf{Y}_j, t_0 + c_j \Delta t). \quad (2.2b)$$

Consistency requires that

$$c_i = \sum_j a_{ij} \quad \text{and} \quad (2.3)$$

$$\sum_j b_j = 1. \quad (2.4)$$

Moreover, for an explicit method, only the strictly lower triangular elements of the matrix a_{ij} come into play (and therefore $c_1 = 0$). It is convenient and has

Corresponding author address: Dr. R. James Purser, W/NP2 RM 207, WWBG, NOAA/NCEP, Auth Road, Camp Springs, MD 20746-4304.
E-mail: jim.purser@noaa.gov

become standard (see, e.g., Butcher 1987) to display the coefficients in array form:

$$\begin{array}{c|ccc} 0 & & & \\ c_2 & a_{21} & & \\ c_3 & a_{31} & a_{32} & \\ \hline & b_1 & b_2 & b_3 \end{array} . \quad (2.5)$$

The starting point in WS for their splitting extension is the three-stage method that we shall denote by “WS3” and which, in the notation of (2.5), possesses the coefficients,

$$\text{WS3} \equiv \begin{array}{c|ccc} 0 & & & \\ \frac{1}{3} & \frac{1}{3} & & \\ \frac{1}{2} & 0 & \frac{1}{2} & \\ \hline & 0 & 0 & 1 \end{array} . \quad (2.6)$$

In the paper by Hundsdorfer et al. (1995) referred to by WS, two third-order Runge–Kutta schemes that they denote RK3a and RK3b are introduced; these are fairly well-known methods attributed, respectively, to Heun (1900) and to Fehlberg (1970) with coefficients

$$\text{RK3a} \equiv \begin{array}{c|ccc} 0 & & & \\ \frac{1}{3} & \frac{1}{3} & & \\ \frac{2}{3} & 0 & \frac{2}{3} & \\ \hline & \frac{1}{4} & 0 & \frac{3}{4} \end{array} , \quad \text{RK3b} \equiv \begin{array}{c|ccc} 0 & & & \\ 1 & 1 & & \\ \frac{1}{2} & \frac{1}{4} & \frac{1}{4} & \\ \hline & \frac{1}{6} & \frac{1}{6} & \frac{2}{3} \end{array} . \quad (2.7)$$

To achieve a third order of accuracy in an explicit three-stage scheme of the form of (2.5), it is shown in Gear (1971, p. 34) and in Butcher (1987, p. 173) that as well as (2.3) and (2.4), the following three additional conditions must hold:

$$R_1 \equiv b_2 c_2 + b_3 c_3 = \frac{1}{2}, \quad (2.8a)$$

$$R_2 \equiv b_2 c_2^2 + b_3 c_3^2 = \frac{1}{3}, \quad \text{and} \quad (2.8b)$$

$$R_3 \equiv b_3 a_{32} c_2 = \frac{1}{6}. \quad (2.8c)$$

While for schemes RK3a and RK3b, all the conditions of (2.3), (2.4), and (2.8a)–(2.8c) are satisfied, we find that for the scheme WS3, condition (2.8b) is violated since

$$R_2^{(\text{WS3})} = \frac{1}{4} \neq \frac{1}{3}. \quad (2.9)$$

It is instructive to examine the consequences of this defect in the context of idealized dynamics where the degree of nonlinearity of the forcing \mathbf{f} as a function of the state $\boldsymbol{\psi}$ is quantifiable and under our control. Such an example is the motion of a particle in a plane at Cartesian coordinates (x, y) influenced by an acceleration $-F_r$ toward the origin, where F_r equals some power p of the radius $r = (x^2 + y^2)^{1/2}$. Thus,

$$\boldsymbol{\psi} \equiv (x, y, u, v), \quad (2.10)$$

and the corresponding forcing terms,

$$\mathbf{f} \equiv (u, v, f, g), \quad (2.11)$$

are as such to satisfy

$$f = -xr^{(p-1)} \quad \text{and} \quad (2.12a)$$

$$g = -yr^{(p-1)}. \quad (2.12b)$$

Selecting $p = 1$ implies linear dynamics and, consequently, harmonic motion; $p = -2$ implies Kepler orbits. However, a state initialized to

$$\boldsymbol{\psi}_0 = (1, 0, 0, 1) \quad (2.13)$$

is analytically integrable and must lead to circular motion,

$$[x(t), y(t)] = [\cos(t), \sin(t)], \quad (2.14)$$

for every choice of the force-law exponent p .

For linear dynamics, $p = 1$, we find that all n -stage Runge–Kutta approximations of the order n for a given time step Δt lead to identical outcomes $\boldsymbol{\psi}(t_0 + \Delta t)$. In this case, the three-stage scheme WS3 will also reproduce the solution of the RK3 methods. However, the approximate solutions that various n -stage schemes yield when $p \neq 1$ are generally distinctly different. This is illustrated in Fig. 1, which shows the solutions obtained with 16 time steps of size ($\Delta t = \pi/16$; i.e., one-half orbit) for the 3 three-stage methods (RK3a, RK3b, and WS3) when $p = -4$. These are compared with the exact solution. For this relatively long time step, the numerical approximations have comparable errors, although the RK3a scheme most closely approximates the exact solution, shown here by the plus symbol at the left terminus of the unlabeled half-orbit. [The Fehlberg scheme, RK3b, is not usually employed as a stand-alone scheme but rather as part of a more sophisticated package with built-in step-size control (Fehlberg 1970; Butcher 1987, p. 305).]

We determine the “order of accuracy” of different schemes by examining the rate at which the error tends

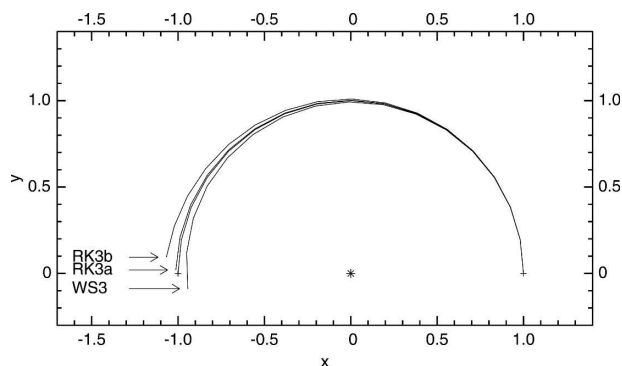


FIG. 1. Comparison of analytic and numerically estimated half-orbits for a central force law with exponent $p = -4$. The numerical schemes WS3, RK3a, and RK3b are compared using 16 time steps. The force is directed toward the asterisk at the center with a magnitude in proportion to r^p , where r is the radial distance. The start and end points of the true trajectory is marked by plus symbols and the end points of the three numerical methods are indicated by the arrows.

to zero when the time step is progressively refined. In the linear dynamics case, $p = 1$, Fig. 2a shows graphs plotted in a log-log framework of the absolute displacement error at the completion of the half-orbit at the time step of Fig. 1 and at six successive bisections of the time step. All of the three-stage schemes now collapse to a common solution, marked here by RK3, giving a graph whose average slope closely approximates the value of 3 expected of schemes having third-order temporal accuracy. For comparison, a second-order “modified Euler” Runge–Kutta scheme denoted “RK2” and the “classical” fourth-order Runge–Kutta scheme “RK4,” possessing the coefficients (Butcher 1987)

$$\text{RK2} \equiv \begin{array}{c|c} 0 & 0 \\ \hline \frac{1}{2} & \frac{1}{2} \\ \hline 0 & 1 \end{array}, \quad \text{RK4} \equiv \begin{array}{c|ccc} 0 & 1 & 2 & 3 \\ \hline \frac{1}{2} & \frac{1}{2} & \frac{1}{2} & \frac{1}{2} \\ \hline 1 & 0 & 0 & 1 \\ \hline \frac{1}{6} & \frac{1}{3} & \frac{1}{3} & \frac{1}{6} \end{array}, \quad (2.15)$$

are both included in this comparison and clearly show the expected slopes of two and four, respectively.

When the dynamics becomes nonlinear, a qualitatively different picture emerges. Figure 2b shows the results with the exponent in the force-law $p = -4$. The slopes of the schemes RK2, RK3a, RK3b, and RK4 show no change from Fig. 1a, although the graphs of the two RK3 schemes are now separate. However, the plot for the scheme WS3 confirms that this method applied

to nonlinear dynamics attains only second-order accuracy. Likewise, an exponent $p = +4$, shown in Fig. 2c, shows a similar separation of the two RK3 methods and a formal second-order of accuracy for the scheme WS3.

3. Lorenz three-cycle schemes

Lorenz (1971) also introduced 2 three-stage “three-cycle” time integration schemes of Runge–Kutta type but with a special construction that offers a simple implementation with optimal storage economy. If we denote his schemes “L3⁺” and “L3[−],” then instead of mechanically implementing the stages of (2.2a) and (2.2b), we can redefine the implementations for each of his particular schemes through the three-stage accumulation of increments, as in the following generic procedure in which the “+” and “−” algorithms differ only in the terms with superscripts “±”:

$$\mathbf{Y}_1 = \boldsymbol{\psi}(t_0), \quad (3.1a)$$

$$\mathbf{G}_1 = \mathbf{f}(\mathbf{Y}_1, t_0), \quad (3.1b)$$

$$\mathbf{Y}_2 = \mathbf{Y}_1 + \frac{\Delta t}{3} \mathbf{G}_1, \quad (3.1c)$$

$$\mathbf{G}_2^\pm = W_2^\pm \mathbf{f}(\mathbf{Y}_2, t_0 + \Delta t/3) + (1 - W_2^\pm) \mathbf{G}_1, \quad (3.1d)$$

$$\mathbf{Y}_3^\pm = \mathbf{Y}_2 + \frac{\Delta t}{3} \mathbf{G}_2^\pm, \quad (3.1e)$$

$$\mathbf{G}_3^\pm = W_3^\pm \mathbf{f}(\mathbf{Y}_3^\pm, t_0 + 2\Delta t/3) + (1 - W_3^\pm) \mathbf{G}_2^\pm, \quad \text{and} \quad (3.1f)$$

$$\boldsymbol{\psi}(t_0 + \Delta t) = \mathbf{Y}_3^\pm + \frac{\Delta t}{3} \mathbf{G}_3^\pm. \quad (3.1g)$$

The weights defining these 2 three-cycle schemes are

$$W_2^+ = W_3^- = 3/2 \quad \text{and} \quad (3.2a)$$

$$W_3^+ = W_2^- = 3. \quad (3.2b)$$

Put into standard form, these two schemes are exactly equivalent to the explicit one-step methods:

$$\text{L3}^+ \equiv \begin{array}{c|cc} 0 & 1 & 2 \\ \hline \frac{1}{3} & \frac{1}{3} & \frac{1}{2} \\ \hline \frac{2}{3} & \frac{1}{6} & \frac{1}{2} \\ \hline \frac{1}{2} & -\frac{1}{2} & 1 \end{array}, \quad \text{L3}^- \equiv \begin{array}{c|cc} 0 & 1 & 2 \\ \hline \frac{1}{3} & \frac{1}{3} & \frac{1}{2} \\ \hline \frac{2}{3} & -\frac{1}{3} & 1 \\ \hline 0 & \frac{1}{2} & \frac{1}{2} \end{array}. \quad (3.3)$$

As Lorenz noted, these schemes also fail to be fully third order. Although they fail to satisfy (2.8b), they are

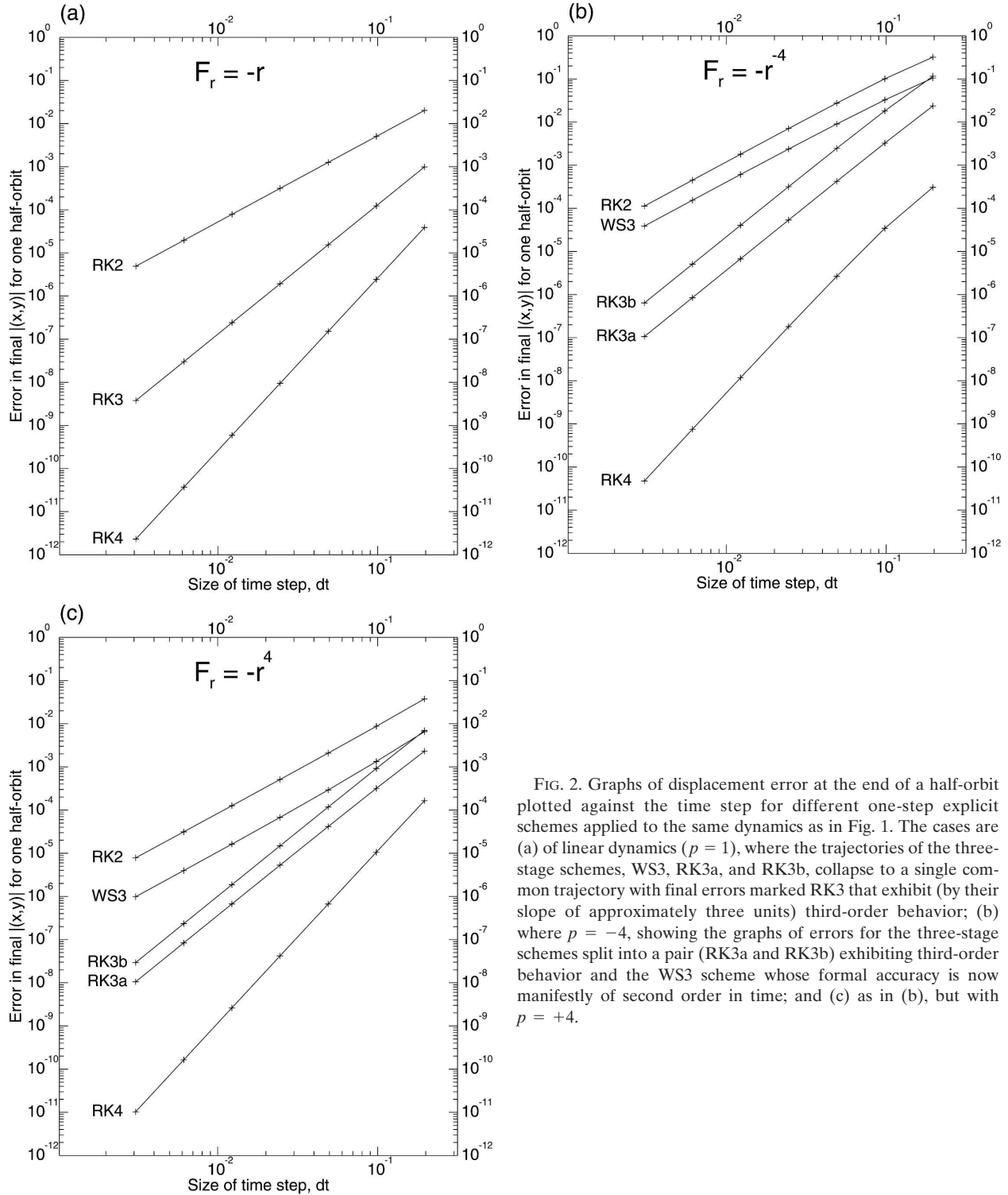


FIG. 2. Graphs of displacement error at the end of a half-orbit plotted against the time step for different one-step explicit schemes applied to the same dynamics as in Fig. 1. The cases are (a) of linear dynamics ($p = 1$), where the trajectories of the three-stage schemes, WS3, RK3a, and RK3b, collapse to a single common trajectory with final errors marked RK3 that exhibit (by their slope of approximately three units) third-order behavior; (b) where $p = -4$, showing the graphs of errors for the three-stage schemes split into a pair (RK3a and RK3b) exhibiting third-order behavior and the WS3 scheme whose formal accuracy is now manifestly of second order in time; and (c) as in (b), but with $p = +4$.

complementary in the sense that their errors in this diagnostic are equal in magnitude but opposite:

$$R_2^{(L3\pm)} = \frac{1}{3} \pm \frac{1}{18}. \quad (3.4)$$

Like the WS3 scheme, the three-cycle methods are actually “three-stage second-order Runge–Kutta” methods that conform to the true RK3 methods only in the special case of linear dynamics. Lorenz suggests that by applying $L3^+$ and $L3^-$ at alternating time steps, a final

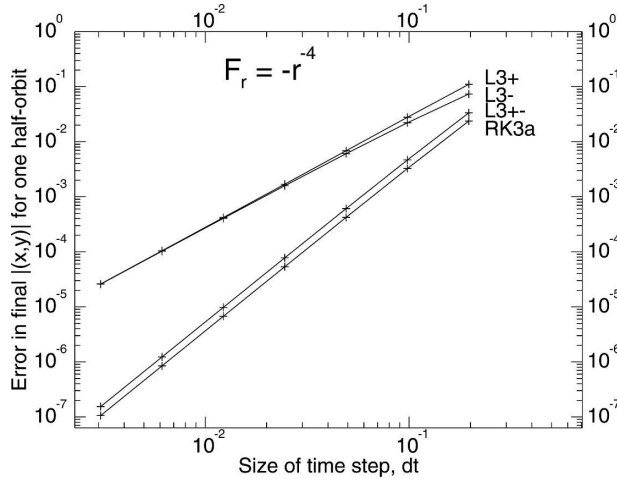


FIG. 3. As in Fig. 2b, but comparing the Lorenz three-cycle schemes ($L3^+$, $L3^-$, and their alternating combination $L3^{+-}$) and the true Runge–Kutta method (RK3a). We see that the alternating combination of Lorenz schemes attains third-order accuracy while the component schemes individually do not.

result of full third order is recovered. Figure 3 supports this conclusion for the case when $p = -4$ where we see that both schemes applied independently exhibit second-order accuracy, while the alternating combination, here labeled $L3^{+-}$, closely matches the performance of the fully third-order Runge–Kutta scheme (RK3a).

Unfortunately, a three-stage scheme does not exist that has an array of coefficients as simple as those of the scheme WS3 that we can take as the “complement” of this scheme in any way that resembles how the pair of Lorenz schemes are mutually complementary. While the Lorenz schemes themselves would also seem to be amenable to a splitting procedure like that described in WS, tests of this approach reported to the author independently (Drs. L. Wicker and J. Sela 2005, personal communication) have not been encouraging; Dr. Louis Wicker notes that the Lorenz schemes do not allow restarts of the substep calculations from the initial time that would enable the fast modes to be properly time centered, leading to a less robust additive splitting method for this combination. The value of centering the calculations in a splitting method has been nicely illustrated in a related context in the recent study by Gassmann (2005), who introduces a scheme that improves upon the stability characteristics of the RK2 scheme of Wicker and Skamarock (1998).

4. Williamson’s low-storage schemes

Another approach to achieving low storage in a third-order Runge–Kutta scheme was taken by Wil-

liamson (1980), whose family of schemes may be written in a way that generalizes the Lorenz schemes by allowing unequal substeps:

$$\mathbf{Y}_1 = \boldsymbol{\psi}(t_0), \quad (4.1a)$$

$$\mathbf{E}_1 = R_1 \mathbf{f}(\mathbf{Y}_1, t_0), \quad (4.1b)$$

$$\mathbf{Y}_2 = \mathbf{Y}_1 + \Delta t \mathbf{E}_1, \quad (4.1c)$$

$$\mathbf{E}_2 = R_2 \mathbf{f}(\mathbf{Y}_2, t_0 + c_2 \Delta t) + Q_2 \mathbf{E}_1, \quad (4.1d)$$

$$\mathbf{Y}_3 = \mathbf{Y}_2 + \Delta t \mathbf{E}_2, \quad (4.1e)$$

$$\mathbf{E}_3 = R_3 \mathbf{f}(\mathbf{Y}_3, t_0 + c_3 \Delta t) + Q_3 \mathbf{E}_2, \quad \text{and} \quad (4.1f)$$

$$\boldsymbol{\psi}(t_0 + \Delta t) = \mathbf{Y}_3 + \Delta t \mathbf{E}_3. \quad (4.1g)$$

Following Kopal (1961), Williamson showed that the substep parameters c_2 and c_3 are coupled by an algebraic constraint. In a form that is equivalent to Williamson’s, but more symmetrically expressed, this constraint emerges by substituting

$$c_2 = 1/X, \quad (4.2a)$$

$$c_3 = 1 - 1/Z, \quad (4.2b)$$

when X and Z are required to satisfy

$$Z^2 \left(1 - X + \frac{X^2}{3} \right) + Z \left(-1 + \frac{3}{2} X - X^2 \right) + (-X + X^2) = 0. \quad (4.3)$$

The other coefficients of the array form [Eq. (2.5)] of each scheme are

$$b_1 = \frac{6c_2c_3 - 3c_3 - 3c_2 + 2}{6c_2c_3}, \quad (4.4a)$$

$$b_2 = \frac{3c_3 - 2}{6c_2(c_3 - c_2)}, \quad (4.4b)$$

$$b_3 = \frac{2 - 3c_2}{6c_3(c_3 - c_2)}, \quad (4.4c)$$

$$a_{21} = c_2, \quad (4.4d)$$

$$a_{31} = \frac{c_3(-3c_2^2 + 3c_2 - c_3)}{c_2(2 - 3c_2)}, \quad (4.4e)$$

$$a_{32} = \frac{c_3(c_3 - c_2)}{c_2(2 - 3c_2)}, \quad (4.4f)$$

or the limiting values of these expressions when their numerators and denominators both go to zero. The weights must satisfy

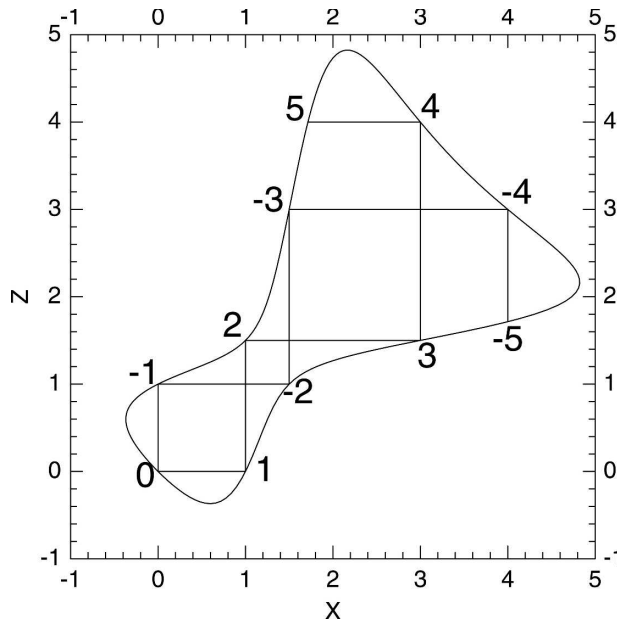


FIG. 4. Locus (curved line) of parameters, $X = 1/c_2$ and $Z = 1/(1 - c_3)$, of third-order Runge–Kutta schemes for which a low-storage implementation is possible. Some of the schemes with simple rational coefficients are included, together with a graphical depiction of the inductive process that generates them as a double-sided sequence. The method recommended by Williamson corresponds to the scheme associated with the point labeled 4.

$$R_1 = c_2, \quad (4.5a)$$

$$R_3 = b_3, \quad (4.5b)$$

$$R_2 = \frac{1}{6R_1R_3}, \quad (4.5c)$$

$$Q_2 = \frac{c_3 - c_2 - R_2}{R_1}, \quad \text{and} \quad (4.5d)$$

$$Q_3 = \frac{b_2}{R_2} - 1. \quad (4.5e)$$

We notice that (i) the left-hand side of (4.3) is symmetrical under the interchange of X and Z , (ii) it is a quadratic in X when Z is fixed and vice versa, (iii) all coefficients of the expression are rational numbers, and (iv) the graph of this constraint contains the (X, Z) origin. As depicted graphically in Fig. 4, these properties together imply by induction the existence of rational-coefficient solutions S_n , forming a two-way sequence with the origin as a member, say S_0 . To show this, we note that given any rational solution $[S_{2p} \equiv (X_{2p}, Z_{2p})]$, the “other” solution at fixed Z to the quadratic in X must also be a rational-coefficient solution [e.g., $S_{2p+1} \equiv (X_{2p+1}, Z_{2p+1})$], where

$$X_{2p+1} = \frac{3(2 - 3Z_{2p} + 2Z_{2p}^2)}{2(3 - 3Z_{2p} + Z_{2p}^2)} - X_{2p}, \quad (4.6a)$$

$$Z_{2p+1} = Z_{2p}, \quad (4.6b)$$

and by symmetrically interchanging X and Z , the same formula supplies the next even-index scheme (S_{2p+2}) in which it is now the X that is held fixed and so on in alternating steps. While the sequence members S_{-1} , S_0 , and S_1 do not translate back into meaningful integration schemes owing to indeterminacies implied by the time step subdivisions, and while less obviously, $S_3 \equiv (3, 3/2)$ cannot form a Runge–Kutta scheme with finite coefficients, all the other members of the sequence do form rational coefficient schemes. Table 1 lists those members of the sequence between S_{-5} and S_5 with their substep parameters, their weights, and the “case numbers” by which Williamson originally identified them.

On the basis of several numerical tests, Williamson (1980) championed the particular scheme here labeled S_4 , whose array coefficients form the tableau,

TABLE 1. Some low-storage RK3 schemes with rational coefficients.

Scheme	Index used by Williamson	X	Z	c_2	c_3	R_1	R_2	R_3	Q_2	Q_3
S_{-5}	5	4	$\frac{12}{7}$	$\frac{1}{4}$	$\frac{5}{12}$	$\frac{1}{4}$	$\frac{2}{9}$	3	$-\frac{2}{9}$	$-\frac{29}{2}$
S_{-4}	6	4	3	$\frac{1}{4}$	$\frac{2}{3}$	$\frac{1}{4}$	$\frac{8}{9}$	$\frac{3}{4}$	$-\frac{17}{9}$	-1
S_{-3}	12	$\frac{3}{2}$	3	$\frac{2}{3}$	$\frac{2}{3}$	$\frac{2}{3}$	$\frac{3}{4}$	$\frac{1}{3}$	$-\frac{9}{8}$	$-\frac{4}{9}$
S_{-2}	4	$\frac{3}{2}$	1	$\frac{2}{3}$	0	$\frac{2}{3}$	$-\frac{3}{4}$	$-\frac{1}{3}$	$\frac{1}{8}$	-2
S_2	14	1	$\frac{3}{2}$	1	$\frac{1}{3}$	1	$\frac{2}{9}$	$\frac{3}{4}$	$-\frac{8}{9}$	$\frac{1}{8}$
S_4	7	3	4	$\frac{1}{3}$	$\frac{3}{4}$	$\frac{1}{3}$	$\frac{15}{16}$	$\frac{8}{15}$	$-\frac{25}{16}$	$-\frac{17}{25}$
S_5	—	$\frac{12}{7}$	4	$\frac{7}{12}$	$\frac{3}{4}$	$\frac{7}{12}$	$\frac{6}{7}$	$\frac{1}{3}$	$-\frac{58}{49}$	$-\frac{1}{3}$

$$S_4 \equiv \begin{array}{c|cc} 0 & & \\ \frac{1}{3} & \frac{1}{3} & \\ \frac{3}{4} & -\frac{3}{16} & \frac{15}{16} \\ \hline & \frac{1}{6} & \frac{3}{10} & \frac{8}{15} \end{array} . \quad (4.7)$$

But it would appear that several of the schemes of Table 1 would be amenable to a splitting treatment to accommodate the fast modes of a model and would then provide truly third-order schemes for the slow modes. While none of these schemes have the conveniently uniform substep size that the Lorenz schemes enjoy, they do achieve fully third-order accuracy over each single cycle of their operation.

Acknowledgments. The author would like to thank Dr. Sajal Kar, Dr. Zavisla Janjić, and Joe Sela for helpful discussions and Dr. Louis Wicker and Prof. Dale Durran for their careful reviews and valuable suggestions.

REFERENCES

- Asselin, R. A., 1972: Frequency filter for time integrations. *Mon. Wea. Rev.*, **100**, 487–490.
- Butcher, J. C., 1987: *The Numerical Analysis of Ordinary Differential Equations*. John Wiley, 512 pp.
- Fehlberg, E., 1970: Klassische Runge-Kutta-formeln vierter und niedrigerer ordnung mit schrittweiten-controlle und ihre anwendung auf wärmeleitungsprobleme. *Computing*, **6**, 61–71.
- Gassmann, A., 2005: An improved two-time-level split-explicit integration scheme for non-hydrostatic compressible models. *Meteor. Atmos. Phys.*, **88**, 23–38.
- Gear, C. W., 1971: *Numerical Initial Value Problems in Ordinary Differential Equations*. Prentice-Hall, 253 pp.
- Heun, K., 1900: Neue methode zur approximativen integration der differential-gleichungen einer unabhängigen veränderlichen. *Z. Math. Phys.*, **45**, 23–38.
- Hundsdoerfer, W., B. Koren, M. van Loon, and J. G. Verwer, 1995: A positive finite-difference advection scheme. *J. Comput. Phys.*, **117**, 35–46.
- Klemp, J. B., and R. B. Wilhelmson, 1978: The simulation of three-dimensional convective storm dynamics. *J. Atmos. Sci.*, **35**, 1070–1096.
- Kopal, Z., 1961: *Numerical Analysis*. 2d ed. John Wiley, 594 pp.
- Lorenz, E. N., 1971: An N -cycle time-differencing scheme for stepwise numerical integration. *Mon. Wea. Rev.*, **99**, 644–648.
- Wicker, L. J., and W. C. Skamarock, 1998: A time-splitting scheme for the elastic equations incorporating second-order Runge–Kutta time differencing. *Mon. Wea. Rev.*, **126**, 1992–1999.
- , and —, 2002: Time-splitting methods for elastic models using forward time schemes. *Mon. Wea. Rev.*, **130**, 2088–2097.
- Williamson, J. H., 1980: Low storage Runge-Kutta schemes. *J. Comput. Phys.*, **35**, 48–56.